Meteorol Atmos Phys (2014) 125:89–101
DOI 10.1007/s00703-014-0322-8

ORIGINAL PAPER

Inter-decadal shift of the prevailing tropical cyclone tracks over the western North Pacific and its mechanism study

Haikun Zhao · Liguang Wu

Received: 26 May 2013 / Accepted: 31 March 2014 / Published online: 16 April 2014

Abstract On the basis of observations and results from the combination of a statistical formation model and a trajectory model, the inter-decadal shift of prevailing TC tracks in the western North Pacific (WNP) are examined. The contributions of the changes in large-scale steering flows and tropical cyclone (TC) formation locations to the observed inter-decadal shift are investigated and their relative importance is determined. This study focuses on two periods, 1965–1986 (ID1) and 1987–2010 (ID2), which are determined based on the abrupt change of the annual category 4 and 5 TC frequency derived from the Bayesian change-point detection analysis. It is found that the models can well simulate the primary features of prevailing TC tracks on the inter-decadal timescale. From ID1 to ID2, a significant decrease in the frequency of TC occurrences is observed over the central South China Sea and well simulated by the models. Areas with a remarkable increase in the TC frequency, which extends from the Philippine Sea to the eastern coast of China and in the west of the WNP basin, are also reasonably simulated. Above changes in the prevailing TC tracks are attributed to (1) intensified cyclonic circulation centered over the western part of China and (2) more westward-southward expansion and intensification of the subtropical high over the WNP. Further analysis reveals that the inter-decadal shift in prevailing TC tracks is mainly resulted from the combined effects of changes in large-scale steering flows and TC formation locations. Although both contribute to the inter-decadal shift in the prevailing TC tracks, changes in large-scale steering flows play a more important role compared to changes in TC formation locations.

Responsible editor: C. Simmer.

H. Zhao (✉) · L. Wu
Pacific Typhoon Research Center, Key Laboratory of Meteorological Disaster of Ministry of Education, Nanjing University of Information Science and Technology, Nanjing 210044, China
e-mail: zhk2004y@nuist.edu.cn

1 Introduction

Most studies of tropical cyclones (TCs) in the western North Pacific (WNP) have been focused on their interannual variations. A general consensus is that El Nino-Southern Oscillation (ENSO) significantly affects TC formation region in the WNP (Chan 1985; Wang and Chan 2002; Zhao et al. 2010). Wang and Chan (2002) found enhanced TC formation in the southeastern quadrant of the WNP basin during strong El Nino years, suggesting a southeastward shift in the mean TC formation location during El Nino years compared to La Nina years. This is mainly due to the increase in sea surface temperature (SST) over the central-eastern Pacific in El Nino years. A number of previous studies have investigated the influence of ENSO on TC tracks, largely in terms of the TC landfall patterns (Saunders et al. 2000; Wang and Chan 2002; Wu and Wang 2004; Wu et al. 2004; Fudeyasu et al. 2006; Camargo et al. 2007; Chan et al. 2012). Saunders et al. (2000) argued that the ENSO had a remarkable impact on the landfall patterns of TCs in Vietnam and the Philippines. Wu et al. (2004) also showed the impact of the ENSO on TC landfall activities in the WNP, East Asia, and Southeast Asia.

In addition to the interannual variations, TC tracks also varied on the inter-decadal time scale (Chan and Shi 1996; Ho et al. 2004; Wu et al. 2005; Liu and Chan 2008; Tu et al. 2009). Ho et al. (2004) compared changes in TC tracks between the two periods of 1951–1979 and 1980–2001. They found that the inter-decadal changes were due to the westward expansion of the North Pacific subtropical high. Liu and Chan (2008) investigated the significant inter-decadal variability of prevailing TC tracks in the WNP during the period 1960–2005. They attributed the TC track variability to changes in large-scale steering flows. Previous studies also suggested that there existed inter-decadal scale modulations, which were caused by changes in environmental factors affecting the TC formation and large-scale steering flows in the WNP basin (Wu et al. 2005; Liu and Chan 2008; Kim et al. 2010).

Despite all these studies about variability in TC activities, few are found in current literature to quantitatively discuss the shift of TC tracks on the inter-decadal scale. In particular, possible effects of changes in TC formation locations and large-scale steering flows on the inter-decadal shift of prevailing TC tracks are not well understood mainly due to the lack of an effective diagnostic tool for quantitatively identifying the relative contributions of changes in large-scale atmospheric circulation versus TC formation locations. Recently, Zhao et al. (2010) quantitatively discussed ENSO influence on the prevailing TC tracks in WNP basin utilizing a TC formation model and a trajectory model. Changes in TC formation locations and impact of large-scale flows on the interannual variability of TC tracks were explored. This study provided a basis for further understanding of the variations in prevailing TC tracks on the inter-decadal scale.

The objective of this study is twofold: (1) to evaluate the capability of the combined model, i.e. a TC formation model and a trajectory model, in the study of TC variations on the inter-decadal timescale; and (2) to address the impact of TC formation locations and large-scale steering flows on the inter-decadal shift of prevailing TC tracks over the WNP basin.

This study is organized as follows: The datasets and the selection of the two epochs are described in Sect. 2. The observed inter-decadal shift in prevailing TC tracks in the WNP basin is described in Sect. 3. The capability of the combined model on the inter-decadal timescale is discussed in Sect. 4. Relative roles of large-scale steering flows and TC formation locations are examined in Sect. 5. Section 6 gives summary and discussion.

2 Data and the selection of two epochs

2.1 Data

The TC best track dataset used in this study is derived from the Joint Typhoon Warming Center (JTWC), including the TC locations, 1-min averaged maximum sustained wind speeds, and the central pressure of the TC at 6-h interval. Only those cases that reach at least tropical storm intensity (1-min averaged maximum sustained wind speed >17.2 m s^{-1}) are selected. Wu and Zhao (2012) indicated that JTWC dataset was more reliable compared to other TC best track datasets available in the WNP basin. Chan (2008) also argued that the intensity records from the JTWC dataset were relatively reliable. The analysis period covers the peak TC season (from July to September) during 1965–2010. The year of 1965 is chosen as the starting year because the satellite monitoring of weather events became routine in 1965 and hence no TC would be missed. We focus on the peak TC season because about 50 % of annual TCs form in the peak TC season. Meanwhile, the environmental circulations during the peak TC season are relatively steady and thus the climatological mean flows during the peak TC season can be taken as the background steering flows (Wu and Wang 2004; Wu et al. 2005).

The monthly mean wind fields derived from the National Centers for Environmental Prediction/National Center for Atmospheric Research (NCEP/NCAR) on a $2.5° \times 2.5°$ grid are used (Kalnay et al. 1996). The large-scale steering flow is defined in this study as the pressure-weighted mean flow from 850 to 300 hPa (Holland 1983). The vertical wind shear is computed as the magnitude of the vector difference shear between 200 and 850 hPa. To quantify the changes in the WNP subtropical high, the monthly geo-potential height extracted from NCEP/NCAR is also used. To evaluate the differences in the mean fields between the two samples, the classic nonparametric test, known as the Wilcoxon-Mann–Whitney test, is used in the present study (Chu 2002; Tu et al. 2009).

2.2 Selection of the two epochs

The number of intense TCs (i.e. categories 4 and 5 in the Saffir-Simpson scale, hereafter Cat45) is only used to determine the two epochs for two reasons. First, a significant increase in the number of Cat45 TCs in the WNP basin over the past four decades was mainly due to the shift in the prevailing TC tracks (Webster et al. 2005; Wu and Wang 2008). Second, Wu and Zhao (2012) pointed out that the Cat45 TC frequency was more sensitive to changes in the large-scale environmental fields such as vertical wind shear and SST compared to other TC intensity indices (i.e. TC number; average TC intensity; peak intensity).

As discussed in previous studies (Chan 2006; Landsea et al. 2006; Landsea 2007; Kossin et al. 2007; Emanuel et al. 2008), uncertainty in historical TC records might lead to inconsistency in the TC intensity records. Hence the number of Cat45 TCs in the WNP basin used in this study may be inflated or spurious. Emanuel (2005, 2007) extensively discussed the evolution in measurement and

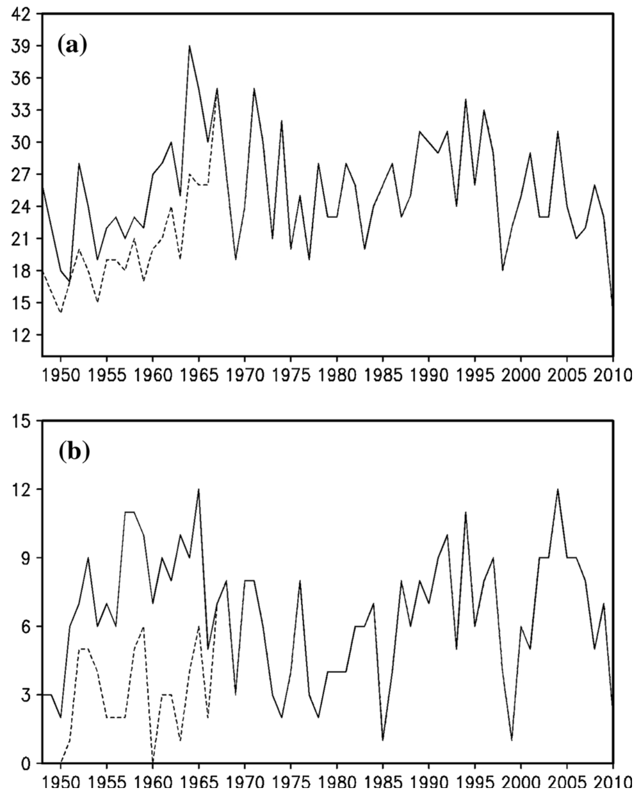

Fig. 1 The annual unadjusted (*solid*) and adjusted (*dashed*) number of tropical cyclones (TCs) reaching tropical storm strength (**a**) and Cat45 TCs (**b**) derived from the Joint Typhoon Warning Center (JTWC) best track dataset over the western North Pacific during the period 1948–2010. TC maximum wind speeds in the JTWC dataset prior to 1973 is adjusted with the pressure-wind relationship as described in Emanuel (2005)

estimation techniques introduced in historical records of TC wind speeds and provided additional evidences supporting the need for a downward adjustment of TC intensities in early records. He proposed the refined combined wind-pressure relationship in Emanuel (2005), which was in agreement with Landsea' s (1993) earlier analysis. In the present study, following Emanuel (2005) (Online supplement), we first adjust the maximum wind speeds in the JTWC dataset prior to 1973. As shown in Fig. 1, the annual TC number is reduced after the adjustment and the annual Cat45 TC frequency is also substantially reduced prior to the 1970s. Recently, the reasonability of this adjusted intensity was justified by using the intensity model developed by Emanuel et al. (2008) in Zhao et al. (2014).

To detect the abrupt shift in tropical cyclone records, a Bayesian change-point analysis (Chu and Zhao 2004; Zhao and Chu 2010) is used for the adjusted Cat45 TC number. Because Cat45 TC occurrence in the WNP basin is regarded as a rare event, a Poisson process is applied to provide a reasonable representation of Cat45 TC frequency. Poisson process is governed by a single parameter, i.e. the

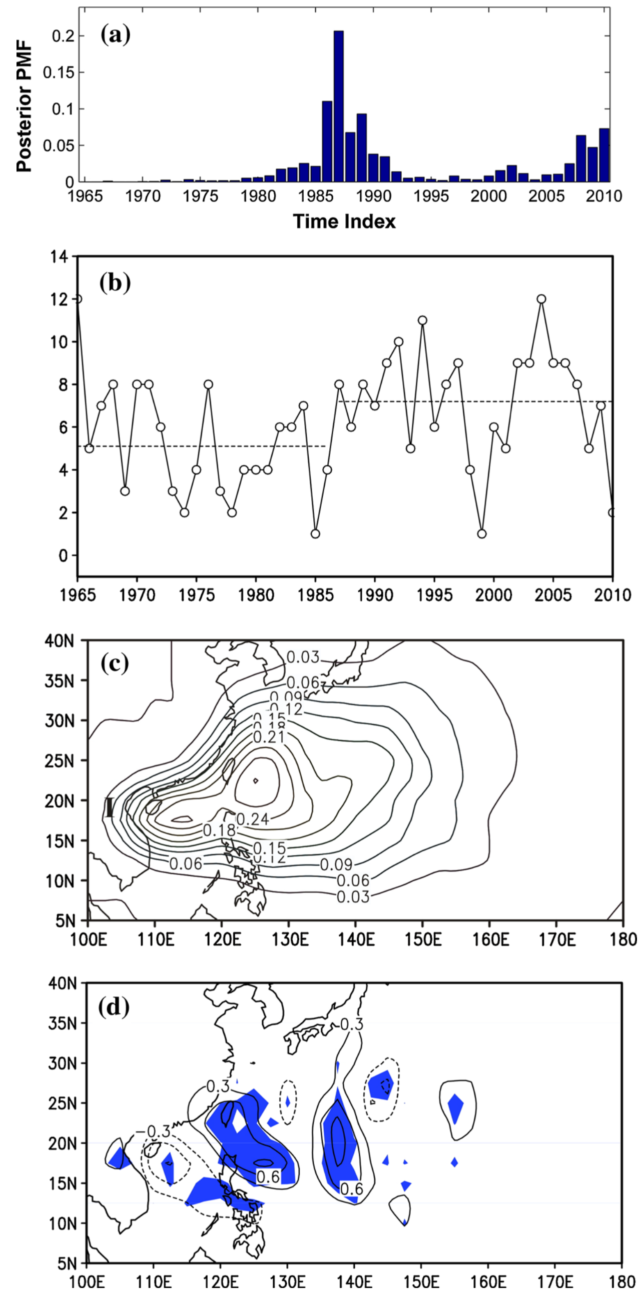

Fig. 2 **a** The conditional posterior probability mass function of change-points is plotted as a function of time. **b** Time series of peak TC season Cat45 TC frequency from 1965 to 2010. **c** Peak season mean frequency of TC occurrence (unit per year-1) derived from the JTWC best track data from 1965 to 2010. **d** Peak season TC frequency differences for the period of 1987–2010 minus the period of 1965–1986. The contours interval is 0.3; *Shading* denotes that the difference the mean of the two epochs is statistically significant at the 5 % level

Poisson intensity. Detailed description can be found in Tu et al. (2009). Figure 2a is the conditional posterior probability mass function of change-points for the time series of seasonal adjusted Cat45 TC frequency over the WNP basin from 1965 to 2010. The interannual variation is relatively small before 1987, but becomes much larger after 1987, indicating a clear shift of TC frequency in 1987. The average number of Cat45 TCs is 5.1 per year during the first epoch (1965–1986), and it becomes 7.2 per year during the second epoch (1987–2010) (Fig. 2b) with an increase of almost 50 % from the first to the second epoch. Furthermore, the difference of the mean Cat45 TC frequencies between the two periods is significant at the 5 % confidence level (Fig. 2b). In addition, the 9-year moving *t* test is applied to the detection of the abrupt inter-decadal change of annual adjusted Cat45 TC counts over the WNP basin from 1965 to 2010. The result indicates that only one significant change can be found in 1987 at the 5 % confidence level (figure not shown). The selection of changing point at 1987 is also consistent with the time of climate regime shift mentioned in the previous studies (Zhang et al. 2008; Wu and Zhang 2007). Wu and Zhang (2007) found that an inter-decadal shift in summer SST variations during the period of 1968–2002 appears in the late 1980s. Zhang et al. (2008) further suggested that a notable decadal shift of the summer climate occurs in eastern China in the late 1980s. In association with this decadal climate shift, the western Pacific subtropical high stretches farther westward with a large south-north extent since late 1980s. Based on above analysis, the study period is divided into two inter-decadal epochs, i.e. 1965–1986 (ID1) and 1987–2010 (ID2), for examining the inter-decadal changes in the prevailing TC tracks over the WNP basin.

3 Observed inter-decadal shift in prevailing TC tracks

In order to further understand the connection between the abrupt shift in Cat45 TC frequency and inter-decadal changes in prevailing TC tracks over the WNP basin, the differences in TC occurrence are calculated for each 2.5° × 2.5° grid box between the two epochs. Note that the all TCs are considered in identifying the three prevailing TC tracks over the WNP basin and investigating the possible cause of the inter-decadal shift in the prevailing TC tracks in this study. The annual Cat45 frequency is just used for determining the two separate epochs.

The prevailing TC tracks are determined based on the frequency of TC occurrences, which are defined at each 2.5° × 2.5° grid box (Wu and Wang 2004). The frequency indicates how often a specific grid box is affected by the TCs. Thus the three prevailing TC tracks can be identified over the WNP from Fig. 2c, which are used as references for examining the TC track changes during the ID1 and ID2. The three prevailing TC tracks can be detected by identifying those grids with a higher TC frequency than their adjacent grids for all years (1965–2010) in the peak TC season. TCs occur most frequently over northern part of South China Sea (SCS) and to the southeast of Taiwan, indicating a prevailing track of the westward-moving TCs (referred to track I). The high-frequency region extending from the Philippine Sea to Korea and Japan suggests another prevailing track that influences the coastal region of East Asian (referred to track II). The third prevailing track is identified with the TCs tending to recurve northeastward east of 130°E (referred to track III), which often happens when WNP subtropical ridge splits. The selection of the three climatological prevailing tracks has little influence on our analyses in this study. Similar application of the prevailing TC tracks for detecting the TC track change is also used by Wu et al. (2005) and Zhao et al. (2010). In addition, we also conduct the cluster analysis of TC tracks. The identified prevailing tracks are nearly identical.

As shown in Fig. 2d, prevailing TC tracks over the WNP exhibit a pronounced shift. Observations of the prevailing TC tracks in the WNP basin show a north-northwestward shift in the second epoch compared to that in the first epoch. An observed sharp decrease of TC frequency from ID1 to ID2 in the central part of South China Sea (SCS) can be found, indicating a northward shift of the previously westward prevailing TC track (track I). Two southeast-northwest extending bands with increased TC frequencies, one from the Philippine Sea to eastern coast of China, and the other in the western part of the WNP basin, indicate significant northwestward shift of the prevailing TC tracks (track II) during ID2. As suggested by Wu and Wang (2008), the abrupt change of intense TC frequency may be closely related to the shift of prevailing TC tracks over the WNP basin. Further studies are necessary to enhance our understanding of connection between Cat45 TC frequency or TC intensity and the prevailing TC tracks over the WNP basin. In this study, we mainly focus on the investigation of the relative impact of large-scale steering flows versus TC formation locations in the inter-decadal shift of prevailing TC tracks in the WNP basin.

4 Capability of the combined model on the study of inter-decadal TC variations

Several statistical models have been developed for studies of TC tracks, including the TCs genesis and their subsequent movements (Darling 1991; Vickery et al. 2000; James and Mason 2005; Hall and Jewson 2007; Rumpf et al. 2007). However, the dynamic process associated with TC activity in the aforementioned studies is not considered. In this study we first utilize a statistical formation model to generate samples of TC formation and then apply a trajectory model to simulate TC tracks. Results of both models are combined to quantify the influence of TC formation locations and large-scale steering flows on the inter-decadal shift of the prevailing TC tracks.

Following Zhao et al. (2010) and Hall and Jewson (2007), the statistical TC formation model is based on the historical TC formation locations during the periods of ID1 and ID2. A two-dimensional (latitude and longitude) probability density function (PDF) is constructed from the observed TC formation information. The formation PDF PDF comprises of sums of kernel about out-of-sample historical genesis sites and takes the form of expression (1). The kernels are Gaussian with anisotropic variance length scales, $\delta_1$and δ_2, which are referred to as the bandwidths of the formation PDF.

$$f(x,y) = \frac{1}{2\pi N\delta_1\delta_2}\sum_{i=1}^{N}\exp\left[\frac{(x-x_i)^2}{2\delta_1^2} - \frac{(y-y_i)^2}{2\delta_2^2}\right], \qquad (1)$$

where N is the numbers of TCs, x_i, y_i are the longitudes and latitudes of historical formation locations, $\delta_1$and $\delta_2$are bandwidths in the latitudinal and longitudinal directions. Here we assume that the direction bandwidths are equal in the longitudinal and latitudinal directions. Formula (1) becomes

$$f(x,y) = \frac{1}{2\pi N\delta^2}\sum_{i=1}^{N}\exp\left[\frac{(x-x_i)^2 + (y-y_i)^2}{2\delta^2}\right]. \qquad (2)$$

To obtain the optimal bandwidths for the two separate inter-decadal periods of ID1 and ID2, the optimal bandwidth needs to be determined from the jackknife out-of-sample likelihood maximization using the cross-validation method. The details can be found in Hall and Jewson (2007). Following this method, the optimal bandwidths are determined to be 2.7° and 2.5° for the period ID1 and ID2, respectively (Fig. 3).

To show the importance of the optimal bandwidth, the kernel PDFs with three different bandwidths for the different epochs are calculated. Figure 4 gives the kernel PDFs with three different bandwidths 0.5°, 2.7°, and 5° for the first epoch ID1. The PDF with bandwidth of 0.5° has a detail structure and gives under-fitted genesis simulation, while the bandwidth of 5° gives over-smoothed simulation and has just one maximum. The intermediate bandwidth of 2.7° is taken as the optimum in the TC peak season during the period 1965–1986, which makes the kernel probability density maximum and captures the historical genesis pattern well (Fig. 5a, b). A similar analysis is performed for the optimal bandwidth of 2.5° in the second epoch ID2 (figures not shown).

Based on the optimal PDFs, TC formation locations can be well simulated with a uniform random number generator. TC formation occurs randomly with a probability given

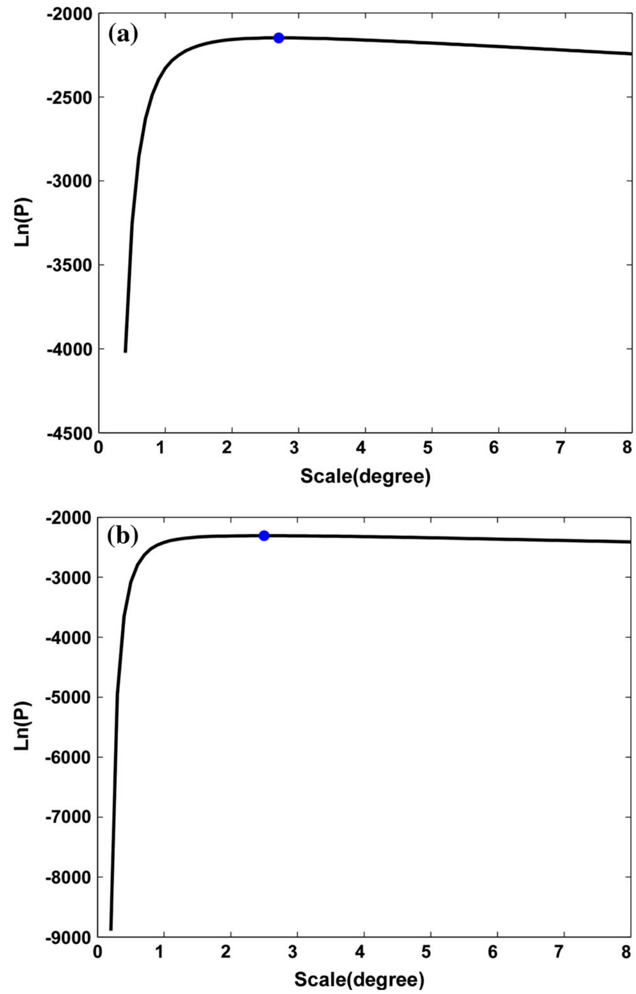

Fig. 3 The out-of-sample log-likehood (y-axis) versus bandwidths (x-axis) for kernel density function described in expression (2). The optimal bandwidths are selected for (**a**) the period **a** ID1 (1965–1986) and **b** ID2 (1987–2010) using a cross-validation method based on the observed information over the peak TC season

by the normalized PDF. A formation location is determined only if it satisfies the observed PDF, respectively, for ID1 and ID2, calculated with Eq. (2). This procedure continues until all of the required formation locations are obtained. The detailed description of generating random number can be found in Hall and Jewson (2007) and Zhao et al. (2010). Ten times as many points as the observed TC formation locations are simulated in this study (Fig. 5). The simulated spatial distributions of the frequency of TC formation agree well with the observation during the period of ID1 and ID2 (Fig. 5a, b, d, e). Further examinations suggested that the pattern correlations between observed and simulated TC genesis distribution are statistically significant with correlation coefficients 0.90 and 0.91, respectively, during ID1 and ID2 periods. In an operational setting, a pattern correlation of 0.60 is deemed as a lower limit for field forecasts that are synoptically useful. Additionally, both the

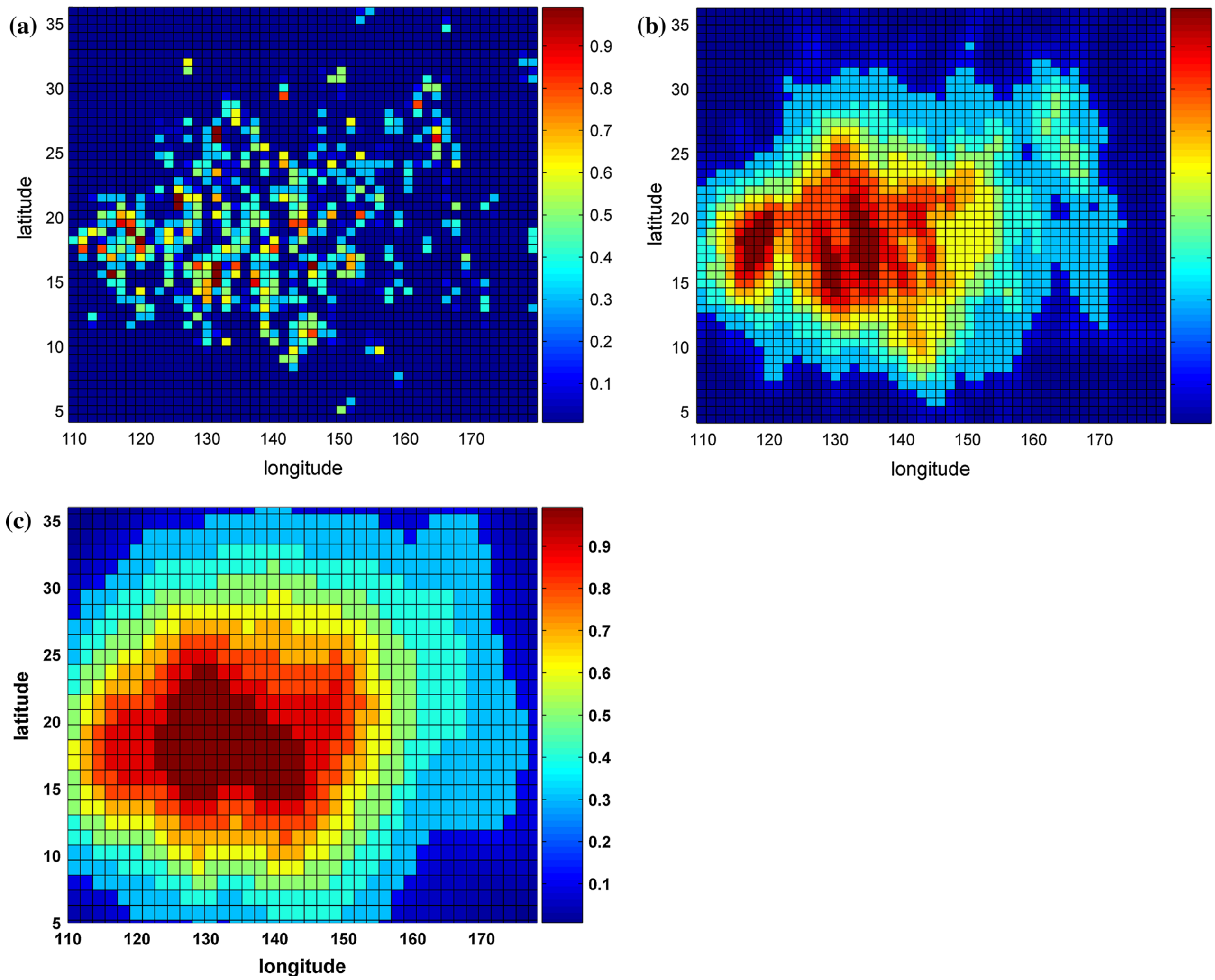

Fig. 4 Guassian kernel formation probability density function (PDF) with bandwidth 0.5° (**a**), 2.7° (**b**), and 5° (**c**) for the period 1965–1986. The PDFs are normalized to the unit maximum

simulations during two periods ID1 and ID2 show a systematically basin-increase, but the difference and their statistical significance between simulated TC genesis and observation during ID1 is generally consistent with that during ID2 (figure not shown). Moreover, the difference and their statistical significance of simulated TC formation between ID1 and ID2 are also compared well with the observation (Fig. 5c, f). In summary, the TC formation model can well simulate the inter-decadal changes in TC genesis over the WNP basin.

The track model is adopted from Wu and Wang (2004). In this model, a TC is taken as a point vortex and moves with the climatological mean steering flow, which is comprised of the pressure-weighted mean flows from 850 to 300 hPa and the mean beta drift. In this study, as in Wang and Wu (2012), random synoptic-scale perturbations are added to mean translation vectors to account for the influence of synoptic scale weather systems, which are not included in Wu and Wang (2004) and Zhao et al. (2010). The variance and spatial distribution of the random perturbations are calculated from the observed synotpical-scale winds. The TC trajectory calculations stop when the TC moves out of the study domain (0–40°N, 100–180°E). As indicated in Table 1, studies of the TC formation locations and large-scale steering flows during the period of ID1 and ID2 are taken as the first and second experiment (hereafter D1D1 and D2D2), respectively.

As shown in Fig. 6, the trajectory model can well simulate the primary changes of the prevailing TC tracks on the inter-decadal timescale based on the climatological TC occurrence distributions during the two inter-decadal periods. Close inspections suggested that both the pattern correlations between simulated and observed TC occurrences during ID1 and ID2, respectively, are statistically significant with correlation coefficients 0.87 and 0.85. Figure 7 shows the difference of the simulated TC

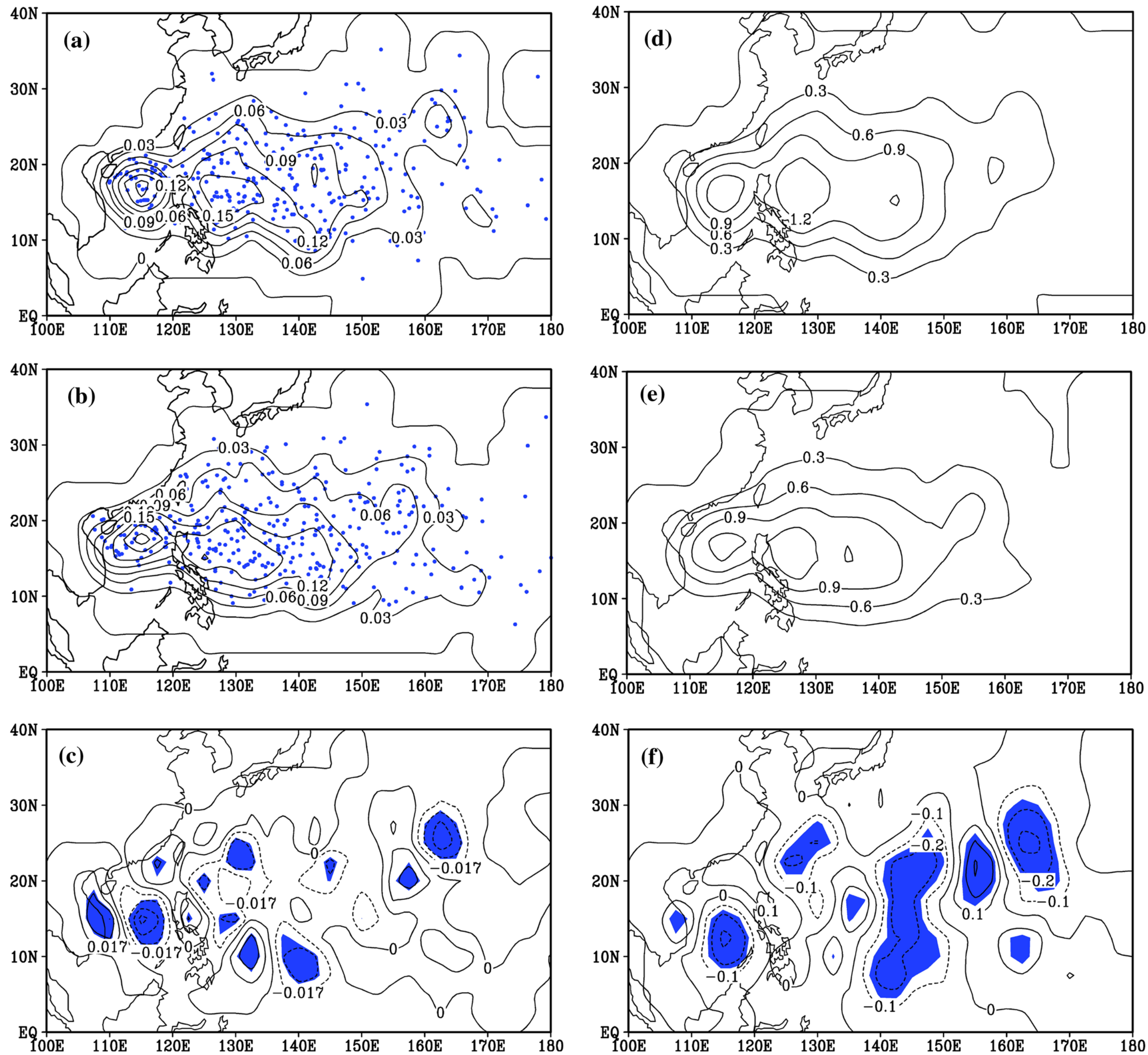

Fig. 5 Spatial distribution of the observed frequency of TC formation locations in the peak TC season for **a** the period 1965–1986, **b** ID1 (1987–2010) and **c** the difference of ID1 and ID2, i.e. (1987–2010) minus (1965–1986). The contour interval is 0.03 decade-1 in (**a**) and (**c**), while 0.01 decade-1 in (**d**). The *closed dots* show simulated TC formation positions. **b**, **e** and **f** are the same as in (**a**), (**b**) and (**c**), but for the simulated TC frequency. In addition, the contour intervals are 0. 3 decade-1 in (**d**) and (**e**), while 0.1 decade-1 in (**f**). *Shading* denotes that the difference the mean of the two epochs is statistically significant at the 5 % level

Table 1 Four experiments and corresponding large scale flows and genesis locations used in each experiment (ID1 1965–1986, ID2 1987–2010)

Experiments	Large-scale steering flows	Genesis locations
D1D1	ID1 period	ID1 period
D2D2	ID2 period	ID2 period
D1D2	ID1 period	ID2 period
D2D1	ID2 period	ID1 period

frequencies between the two experiments D1D1 and D2D2. As shown in Figs. 2d and 7, it is found that the simulated and observed spatial distribution exhibits a pronounced increase of TC frequency, which extends from the Philippine Sea to the eastern coast of China and in the west of the WNP basin (100–140°E), and a significant decrease over the SCS, indicating that the model can simulate the north-northwestward shift of TC frequency since 1987. The areas with a significance level at the 5 % are also almost consistent. However, the magnitude of difference and their

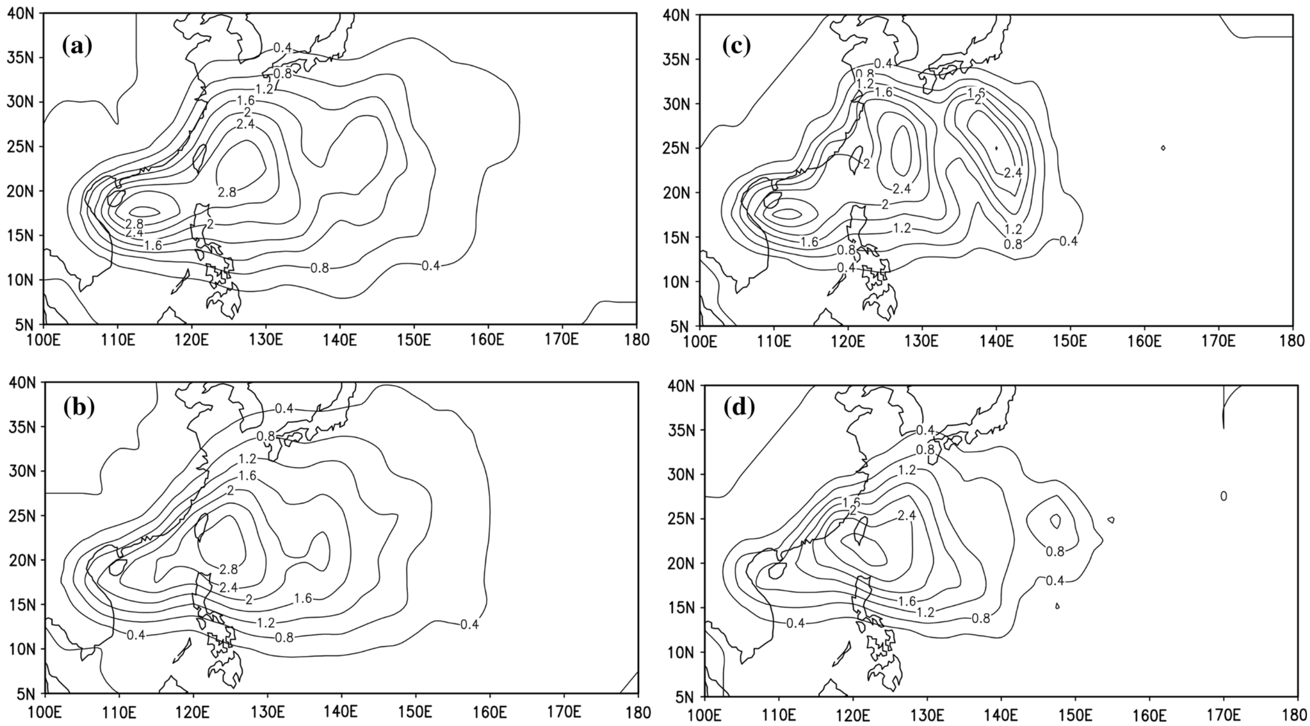

Fig. 6 The average observed (**a** ID1 (1965–1986); **b** ID2 (1987–2010)) and simulated (**c** ID1 (1965–1986); **d** ID2 (1987–2010)) frequency of TC occurrences at a grid of 2.5° × 2.5° in the peak TC season with contour intervals of 0.4

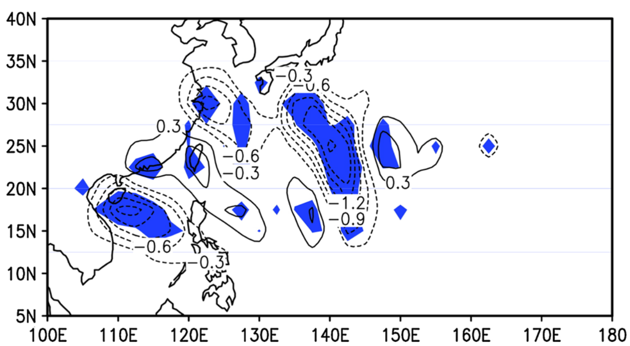

Fig. 7 Simulated differences in the frequency of TC occurrences in the peak TC season between ID1 (1965–1986) and ID2 (1987–2010). The contour interval is 0.3 $year^{-1}$. *Shading* denotes that the difference the mean of the two epochs is statistically significant at the 5 % level

patterns show some discrepancies especially over the east of 140°E in the WNP basin. These biases in model simulations are also mainly due to the insufficient capability of the combined model. For example, the TC formation model is a statistical model, in which dynamic factors affecting TC formation are not considered. Only two main factors are considered in the track model, while previous studies suggested that many other factors (e.g. vertical wind shear, Shapiro 1992; Wu and Emanuel 1993; Wang and Holland 1996; Binary interaction, Lander and Holland 1993) can affect TC track. In general, the trajectory model can successfully simulate the difference in the frequency of TC occurrence between ID1 and ID2, especially for the north-northwestward shift of TC tracks over western part of the WNP basin including the SCS. These results give us confidence to further explore the dynamics behind the observed pronounced inter-decadal north-northwestward shift of prevailing TC tracks over the WNP basin.

5 Impact of large-scale steering flows versus that of TC formation locations

Previous studies suggested that the mean translation speed was the sum of the climatologic mean large-scale steering flow and beta drift (Holland 1983; Wu and Wang 2004). The beta drifts in the two inter-decadal epochs are derived as the difference between the translation vectors and large-scale steering flows (figure not shown). Although large-scale environmental flows can affect beta drift (Smith 1991; Williams and Chan 1994; Wang and Li 1995; Li and Wang 1996; Wang et al. 1997, Zhao et al. 2009), the differences of the beta drift between ID1 and ID2 are found to be very small in this case, suggesting that the inter-decadal changes in translation vectors are dominated by changes in large-scale steering flow. As discussed in Sect. 3, the observed inter-decadal shifts in the prevailing TC tracks between ID1 and ID2 are a combined result of the changes in both large-scale steering flows and TC formation locations (Fig. 7). But what are the relative contributions of TC formation locations versus large-scale steering flows to the observed inter-decadal shift in the prevailing TC tracks over the WNP basin?

To investigate their respective contributions to the observed inter-decadal changes in the prevailing TC tracks, two additional experiments (D1D2 and D2D1) are conducted (Table 1) using the similar method described in Zhao et al. (2010). As mentioned above, it is found that the inter-decadal shift of prevailing TC tracks over the WNP basin are mainly controlled by changes in two factors: their formation locations and large-scale steering flows. To further explore the respective impacts of the large-scale steering flows and TC formation locations on the prevailing TC track change, we combine the TC formation model and track model. The interpretation of the relative roles of changes in TC formation locations and large-scale steering flows is mainly in terms of the track shift pattern and the corresponding magnitudes in the present study. In the experiment D1D2, the large-scale steering flows are obtained from reanalysis for the period ID1 (1965–1986), the TC formation locations are obtained from formation model simulation for ID2 (1987–2010). In the experiment D2D1, the large-scale steering flows are obtained from reanalysis for the period ID2 (1987–2010) and the other input TC formation locations from model simulation during ID1 (1965–1986).

Figure 8a and b illustrates the influence of changes in large-scale steering flows while the TC formation locations remain unchanged. The simulated difference in TC frequencies between experiments D2D1 and D1D1 (Fig. 8a) and that between experiments D2D2 and D1D2 (Fig. 8b) have similar spatial patterns. This pattern implies that the TCs with the prevailing track II (west-northward track) in ID1 now tend to be more westward in ID2. Meanwhile, TCs with the prevailing track I (westward track) in ID1 now tend to be more northward in ID2. Obviously, Fig. 8a and b suggests that the enhanced or decreased TC activities mainly result from changes in large-scale steering flows, which lead to significant increases in the TC frequencies along the eastern coast of China and remarkable decreases in TC occurrence over the SCS. Similarly, the influence of TC formation location is investigated by the simulated differences in the TC frequencies between D1D2 and D1D1 (Fig. 8c) and between D2D2 and D2D1 (Fig. 8d), in which the TC formation locations are changed while the large-scale steering flows remain unchanged. Although the magnitudes of the differences in Fig. 8c and d are significantly smaller than that in Fig. 8a and b, spatial patterns of changes in the TC frequencies are quite similar to that shown Fig. 8a and b. These indicate that changes in TC formation location between ID1 and ID2 also contribute to the inter-decadal shift of TC tracks over the WNP basin.

However, despite the fact that both changes of large-scale steering flows and TC formation locations contribute to changes in prevailing TC tracks, results of above four experiments clearly show that changes of large-scale steering flows play a more important role than that of TC formation locations in terms of the magnitudes of changes in TC frequencies (Fig. 8). Therefore, the inter-decadal changes of the prevailing TC tracks between two periods ID1 and ID2 are mainly due to the changes in the large-scale steering flows, which are characterized by cyclonic circulation centered over the eastern part of China (Fig. 9). This result is consistent with that of Ho et al. (2004) and Chu et al. (2012). Wu et al. (2005) also found westerly flow anomalies to the south of 25°N during 1965–1983 when compared to 1984–2003. Furthermore, to quantify the changes in the western North Pacific subtropical high (WPSH), the WPSH by the contour line for 5,870 gpm of geo-potential height at 500 hPa is also measured, which was also used for examining the changes in WPSH in Zhou et al. (2009). It is found that the subtropical high over WNP basin in the peak TC season expands more westward and southward and intensifies during the period ID2 than ID1 (Fig. 10). These changes in synoptic-scale circulation pattern corresponds to the observed inter-decadal changes in the prevailing TC tracks between ID1 and ID2, especially in the west of 150°E in the WNP basin. Further examination also reveals that the enhanced cyclonic steering flows are attributed to the upper-level circulation change (e.g. 500 hPa) (Figs. 9, 10).

Note that the contributions of changes in TC formation locations to the observed inter-decadal shift of prevailing TC tracks in this study should not assessed totally because it also include the changes in TC number. Further examination suggested the changes in TC number play a relatively minor role in the shift of prevailing TC tracks over the WNP basin. The average number of TCs is 14 per year during the first epoch (1965–1986), and it becomes 14.5 per year during the second epoch (1987–2010) with an increase of only about 4 % from the first to the second epoch. The difference of the mean TC frequencies between the two epochs is not significant at the 5 % confidence level. Also when the combination of the TC formation model and the trajectory model is used for the other scenario, more caution should be paid to the role of the changes in TC number.

6 Summary and discussion

Although changes in TC formation locations and large-scale steering flows both contribute to changes of the

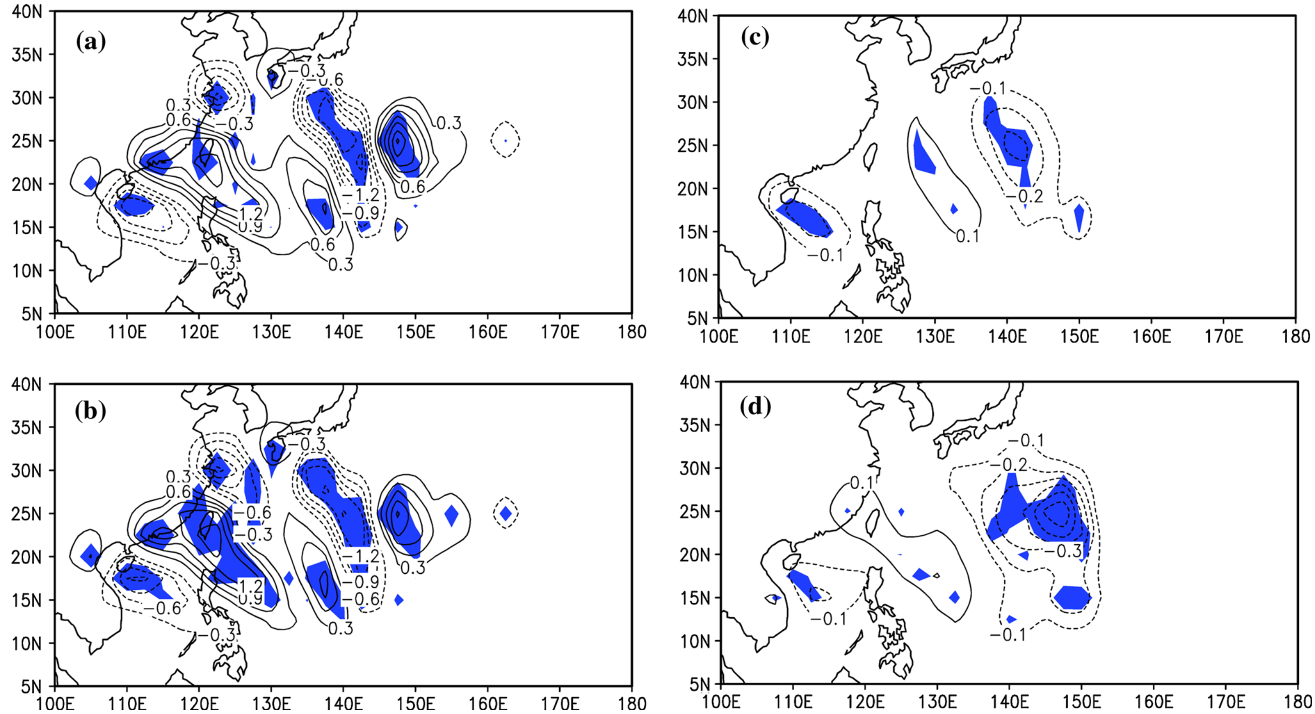

Fig. 8 Simulated differences in the frequency of TC occurrences in the peak TC season between **a** D1D2 and D2D2, **b** D1D1 and D1D2, **c** D2D1 and D2D2, and **d** D1D1 and D2D1, indicating the influences of changes in large-scale steering flows (**a**, **b**) and formation locations (**c**, **d**), respectively. *Shading* indicates the difference is statistically significant at the 5 % confidence level

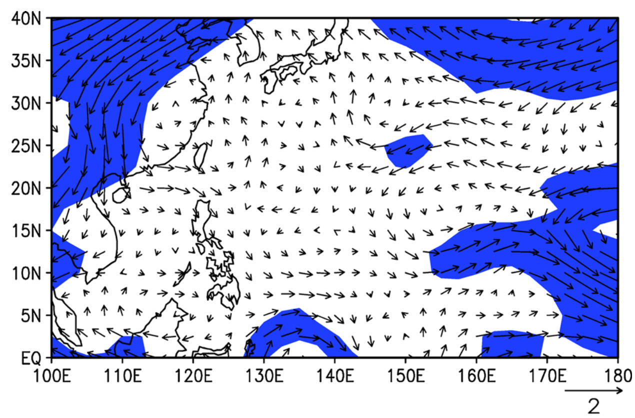

Fig. 9 The difference of large-scale steering flows over the peak TC season between ID1 (1965–1986) and ID2 (1987–2010) derived from the NCEP/NCAR reanalysis data. The unit of the vector is ms^{-1}. *Shading* indicates the difference is statistically significant at the 5 % confidence level

prevailing TC tracks on the inter-decadal timescale, their relative importance has not been well examined. One possible reason is the lack of adequate tools for diagnosing the inter-decadal shift in prevailing TC tracks. In this study, the contributions of these two factors are quantitatively identified by unitizing a statistical formation model and a trajectory model.

To understand the impact of changes in large-scale steering flow and TC formation location on the abrupt inter-decadal shift of the prevailing TC tracks over the WNP basin, two epochs, i.e. 1965–1986 (ID1) and 1987–2010 (ID2), are selected for this study based on the abrupt change of the annual adjusted Cat45 TC frequency. Bayesian change-point analysis clearly shows an abrupt change in the frequency of Cat45 TCs in 1987 when the period of 1965–2010 is examined over the WNP basin. The simulations performed in this study using the statistical formation and track models suggest that the inter-decadal shift in prevailing TC track over the WNP basin is mainly caused by the combined effects of changes in TC formation location and large-scale steering flow between ID1 and ID2. Changes in large-scale steering flow are featured by the westward-southward expansion and intensification of the North Pacific subtropical high. Further analyses in this study suggest that, for the western part of WNP basin, effect of changes in the large-scale steering flow plays a dominant role in changes of prevailing TC tracks, while changes in TC formation location also make their contributions. Our results are consistent with the fact that the increase in Cat45 TCs in the WNP basin over the past four decades is highly associated with the shift of prevailing TC tracks (Wu and Wang 2008).

Additionally, a clear upward trend of global SST is found (figure not shown) during 1965–2010, which is consistent to the global warming found in the previous studies (Trenberth et al. 2007). The spatial distribution of

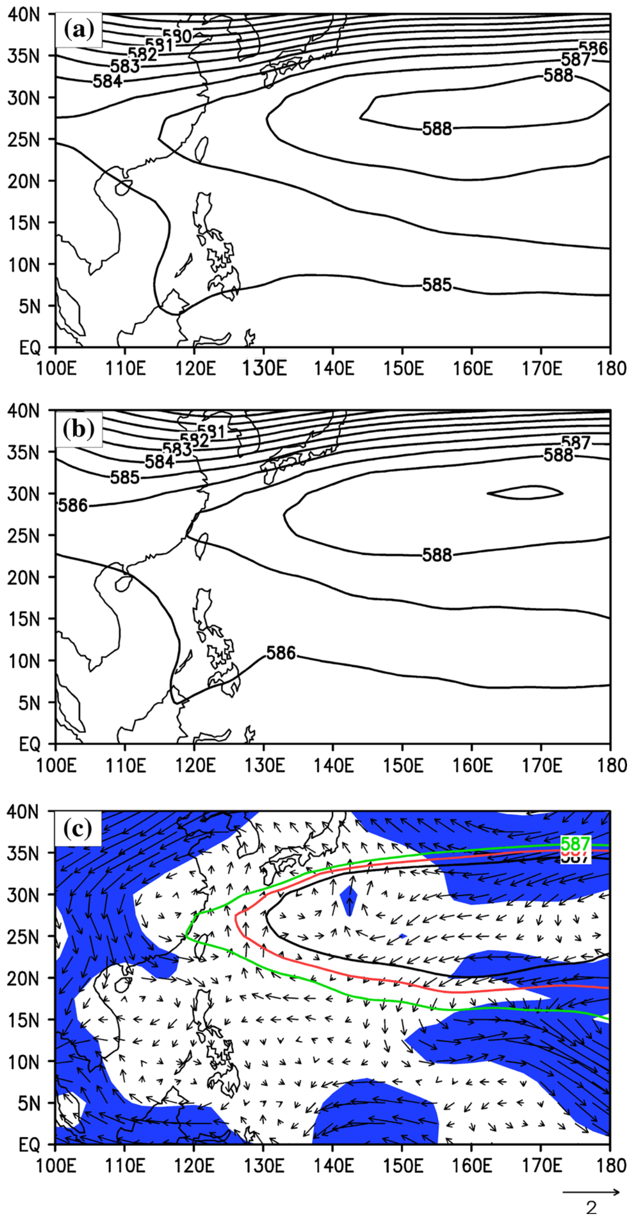

Fig. 10 500 hPa geo-potential height for ID1 (1965–1986) and ID2 (1987–2010) is shown in (**a**) and (**b**) respectively. **c** Difference of wind vectors in 500 hPa between the two epochs ID1 and ID2 are overlapped with the contour lines for 5,870 gpm of 500-hPa geopotential height over the peak TC season. *Black*, *red* and *green lines* indicate the mean position of 5,870 contour for the ID1, climatology (1965–2010) and ID2 respectively. The unit of the vector and the contour, respectively, is ms^{-1} and 10 gpm. *Shading* indicates the difference is statistically significant at the 5 % confidence level

the global SST trend also resembles the SST anomalies related to global warming shown in Wang et al. (2011). Apparently the cyclonic circulation centered over the eastern part of China is related to the global warming and can induce the shift of the TC track over the WNP basin. Based on numerical model results of global warming experiments, Wu and Wang (2004) had suggested that the ongoing global climate change would cause the shift of prevailing TC tracks. These studies implied that a global warming trend of SST could at least be partially responsible for the abrupt shift of the TC tracks over the WNP basin.

The present study implies that the TC formation locations and tracks, which are closely related to TC intensity forecasts, may be affected by global warming. Hence the changes in TC intensity are highly correlated with the changes in SST and the associated variations in adiabatic heating. This issue has been extensively discussed in previous studies (Emanuel 2005; Webster et al. 2005; Landsea 2005, 2007; Hoyos et al. 2006; Chan 2006; Holland and Webster 2007). However, some other studies suggest that the observed changes in TC intensity may not be solely attributed to the local thermodynamic effect of underlying warming SST (Knutson and Tuleya 2004; Emanuel 2005; Webster et al. 2005; Curry et al. 2006), which is inconsistent with the MPI theories (Emanuel 1987; Holland 1997). Up to date, questions of whether the changes in TC activities are due to global warming and whether the global warming trend of SST is induced by anthropogenic forgings still remain unanswered and need further in-depth studies.

It should also be noted that TC activity varies on the interannual, interseasonal, and longer timescale, but the temporal variability is not considered in the statistical formation model. While the climatological beta drifts in this study compare well with the previous numerical results and observations in terms of the magnitudes and directions (Holland 1983; Chan and Williams 1987; Fiorino and Elsberry 1989; Zhao et al. 2009), previous studies have revealed that large-scale environmental flows can significantly affect beta drift (Smith 1991; Williams and Chan 1994; Wang and Li 1995; Wang and Holland 1996; Zhao et al. 2009). These issues should need further study.

Acknowledgments The author thanks Dr. Liguang Wu and Dr. Pao-Shin Chu for valuable comments on the earlier version of this manuscript. This research was jointly supported by the National Natural Science Foundation of China (41305050), the Natural Science Foundation of China (41275093), the National Natural Science Foundation of China (41375098), the foundation of Key Laboratory of Meteorological Disaster of Ministry of Education (KLME1204) and the Priority Academic Program Development of Jiangsu Higher Education Institutions (PAPD).

References

Camargo SJ, Robertson AW, Gaffney SJ et al (2007) Cluster analysis of typhoon tracks. Part I: General properties. J Clim 20(14):3635–3653

Chan JCL (1985) Tropical cyclone activity in the northwest Pacific in relation to the El Niño/Southern Oscillation phenomenon. Mon Weather Rev 113(4):599–606

Chan JCL (2006) Comment on "Changes in tropical cyclone number, duration and intensity in a warming environment". Science 311(5768):1713b

Chan JCL (2008) Decadal variations of intense typhoon occurrence in the western North Pacific. Proc Royal Soc A 464:249–272

Chan JCL, Shi J (1996) Long-term trends and interannual variability in tropical cyclone activity over the western North Pacific. Geophys Res Lett 23(20):2765–2767

Chan JCL, Williams RT (1987) Analytical and numerical studies of the beta-effect in tropical cyclone motion. Part I: zero mean flow. J Atmos Sci 44(9):1257–1265

Chan JC, Liu KS, Xu M, Yang Q (2012) Variations of frequency of landfalling typhoons in East China, 1450–1949. Int J Climatol 32(13):1946–1950

Chu PS (2002) Large-scale circulation features associated with decadal variations of tropical cyclone activity over the central North Pacific. J Clim 15(18):2678–2689

Chu PS, Zhao X (2004) Bayesian change-point analysis of tropical cyclone activity: the Central North Pacific Case. J Clim 17(24):4893–4901

Chu PS, Kim JH, Ruan Chen Y (2012) Have steering flows in the western North Pacific and the South China Sea changed over the last 50 years? Geophys Res Lett 39(10):L10704. doi:10.1029/2012GL051709

Curry JA, Webster PJ, Holland GJ (2006) Mixing politics and science in testing the hypothesis that greenhouse warming is causing a global increase in hurricane intensity. Bull Am Meteorol Soc 87(8):1025–1037

Darling R (1991) Estimation probabilities of hurricane wind speeds using a large-scale empirical model. J Clim 4:1035–1046

Emanuel K (1987) The dependence of hurricane intensity on climate. Nature 326:483–485

Emanuel K (2005) Increasing destructiveness of tropical cyclones over the past 30 years. Nature 436:686–688

Emanuel K (2007) Environmental factors affecting tropical cyclone power dissipation. J Clim 20:5497–5509

Emanuel K, Sundararajan R, Williams J (2008) Hurricanes and global warming: results from downscaling IPCC AR4 simulations. Bull Am Meteorol Soc 89(3):347–367

Fiorino M, Elsberry RL (1989) Some aspects of vortex structure related to tropical cyclone motion. J Atmos Sci 46:975–990

Fudeyasu H, Iizuka S, Matsuura T (2006) Impact of ENSO on landfall characteristics of tropical cyclones over the western North Pacific during the summer monsoon season. Geophys Res Lett 33:L21815. doi:10.1029/2006GL0277449

Hall TM, Jewson S (2007) Statistical modeling of North Atlantic tropical cyclone tracks. Tellus A 5:486–498

Ho CH, Baik JJ, Kim JH, Gong DY, Sui CH (2004) Interdecadal changes in summertime typhoon tracks. J Clim 17:1767–1776

Holland GJ (1983) Tropical cyclone motion: environmental interaction plus a beta effect. J Atmos Sci 40:338–342

Holland GJ (1997) The maximum potential intensity of tropical cyclone. J Atmos Sci 54:2519–2541

Holland GJ, Webster PJ (2007) Heightened tropical cyclone activity in the North Atlantic: natural variability or climate trend? Phil Trans R Soc A. doi:10.1098/rsta.2007.2083

Hoyos CD, Agudelo PA, Webster PJ, Curry JA (2006) Deconvolution of the factors contributing to the increase in global hurricane intensity. Science 312:94–97

James MK, Mason LB (2005) Synthetic tropical cyclone database. J Waterw Port Coast Ocean Eng 131(4):181–192

Kalnay E, Kanamitsu M, Kistler R et al (1996) The NCEP/NCAR 40-year reanalysis project. Bull Am Meteorol Soc 77(3):437–471

Kim JH, Ho CH, Chu PS (2010) Dipolar redistribution of summertime tropical cyclone genesis between the Philippine Sea and the northern South China Sea and its possible mechanisms. J Geophys Res 115:D06104. doi:10.1029/2009JD012196

Knutson TR, Tuleya RE (2004) Impact of CO2-induced warming on simulated hurricane intensity and precipitation: sensitivity to the choice of climate model and convective parameterization. J Clim 17(18):3477–3495

Kossin JP, Knapp KR, Vimont DJ, Murnane RJ, Harper BA (2007) A globally consistent reanalysis of hurricane variability and trends. Geophys Res Lett 34:L04815. doi:10.1029/2006GL028836

Lander M, Holland GJ (1993) On the interaction of tropical-cyclone-scale vortices. I: observations. Q J Roy Meteorol Soc 119(514):1347–1361

Landsea CW (1993) A climatology of intense (or major) Atlantic hurricanes. Mon Weather Rev 121(6):1703–1713

Landsea CW (2005) Hurricanes and global warming. Nature 438:E11–13. doi:10.1038/nature04477

Landsea C (2007) Counting Atlantic tropical cyclones back to 1900. Eos Trans Am Geophys Union 88(18):197–202

Landsea CW, Harper BA, Hoarau K, Knaff JA (2006) Can we detect trends in extreme tropical cyclones? Science 313:452–454

Li X, Wang B (1996) Acceleration of the hurricane beta drift by shear strain rate of an environmental flow. J Atmos Sci 53(2):327–334

Liu KS, Chan JCL (2008) Interdecadal variability of western North Pacific tropical cyclone tracks. J Clim 21(17):4464–4476

Rumpf J, Weindl H, Hoppe P, Rauch E, Schmidt V (2007) Stochastic modeling of tropical cyclone tracks. Math Meth Oper Res 66:475–490

Saunders MA, Chandler RE, Merchant CJ et al (2000) Atlantic hurricanes and NW Pacific typhoons: ENSO spatial impacts on occurrence and landfall. Geophys Res Lett 27(8):1147–1150

Shapiro LJ (1992) Hurricane vortex motion and evolution in a three-layer model. J Atmos Sci 49:140–153

Smith RK (1991) An analytic theory of tropical cyclone motion in a barotropic shear flow. Quart J Roy Meteorol Soc 117:685–714

Trenberth KE, Jones PD, Ambenje P, Bojariu R, Easterling D, Klein Tank A, Parker D, Rahimzadeh F, Renwick JA, Rusticucci M, Soden B, Zhai P (2007) Observations: surface and atmospheric climate change. In: Solomon S, Qin D, Manning M, Chen Z, Marquis MC, Averyt KB, Tignor M, Miller HL (eds) Climate change 2007. The physical science basis. Intergovernmental panel on climate change. Cambridge University Press, Cambridge, pp 235–336

Tu JY, Chou C, Chu PS (2009) The abrupt shift of typhoon activity in the vicinity of Taiwan and its association with western North Pacific-East Asian climate change. J Clim 22:3617–3628

Vickery PJ, Skerlj PF, Twisdale LA (2000) Simulation of hurricane risks in the US using an empirical track model. J Struct Eng 126:1222–1237

Wang B, Chan JCL (2002) How strong ENSO events affect tropical storm activity over the western North Pacific. J Clim 15(13):1643–1658

Wang Y, Holland GJ (1996) Tropical cyclone motion and evolution in vertical shear. J Atmos Sci 53:3313–3332

Wang B, Li X (1995) Propagation of a tropical cyclone in a meridionally varying zonal flow: an energetics analysis. J Atmos Sci 52(9):1421–1433

Wang C, Wu L (2012) Tropical cyclone intensity in the Western North Pacific: downscaling from IPCC AR4 experiments. J Meteorol Soc Jpn 90(2):223–233

Wang B, Li X, Wu L (1997) Direction of hurricane beta drift in horizontally sheared flows. J Atmos Sci 54(11):1462–1471

Wang R, Wu L, Wang C (2011) Typhoon track changes associated with global warming. J Clim 24:3748–3752

Webster PJ, Holland GJ, Curry JA et al (2005) Changes in tropical cyclone number, duration, and intensity in a warming environment. Science 309(5742):1844–1846

Williams RT, Chan JCL (1994) Numerical studies of the beta effect in tropical cyclone motion. Part II: zonal mean flow effects. J Atmos Sci 51:1065–1076

Wu CC, Emanuel K (1993) Interaction of a baroclinic vortex with background shear: application to hurricane movement. J Atmos Sci 50:62–76

Wu L, Wang B (2004) Assessing impacts of global warming on tropical cyclone tracks. J Clim 17:1686–1698

Wu L, Wang B (2008) What changed the proportion of intense hurricanes in the last 30 years? J Clim 21:1434–1441

Wu B, Zhang R (2007) Interdecadal shift in the western North Pacific summer SST anomaly in the late 1980s. Chin Sci Bull 52(18):2559–2564

Wu L, Zhao H (2012) Dynamically derived tropical cyclone intensity changes over the Western North Pacific. J Clim 25(1):89–98

Wu MC, Chang WL, Leung WM (2004) Impacts of El Niño-Southern Oscillation events on tropical cyclone landfalling activity in the western North Pacific. J Clim 17(6):1419–1428

Wu L, Wang B, Geng S (2005) Growing influence of typhoon on East Asia. Geophys Res Lett 32:L18703. doi:10.1029/2005GL022937

Zhao H, Wu L, Zhou W (2010) Assessing the influence of the ENSO on tropical cyclone prevailing tracks in the Western North Pacific. Adv Atmos Sci 27:1361–1371. doi:10.1007/s00376-010-9161-9

Zhang R, Wu B, Zhao P (2008) The decadal shift of the summer climate in the late 1980s over Eastern China and its possible causes. Acta Meteorologica Sinica 22(4):435–445

Zhao X, Chu PS (2010) Bayesian change point analysis for extreme events (typhoons, heavy rainfall, and heat waves): an RJMCMC approach. J Clim 23(5):1034–1046

Zhao H, Wu L, Zhou W (2009) Observational relationship of climatologic beta drift with large-scale environmental flows. Geophys Res Lett 36:L18809. doi:10.1029/2009GL040126

Zhao H, Wu L, Wang R (2014) Decadal variations of intense tropical cyclones over the Western North Pacific during 1948–2010. Adv Atmos Sci 31(1):57–65

Zhou T, Yu R, Zhang J, Drange H, Cassou C, Deser C, Okumura Y (2009) Why the western Pacific subtropical high has extended westward since the late 1970s. J Clim 22(8):2199–2215